DNA polyhedra with T-linkage

ARTICLE *in* ACS NANO · MAY 2012

Impact Factor: 12.88 · DOI: 10.1021/nn300813w · Source: PubMed

DNA Polyhedra with T-Linkage

Xiang Li,[†] Chuan Zhang,[†] Chenhui Hao,[†] Cheng Tian,[†] Guansong Wang,[‡,*] and Chengde Mao[†,*]

[†]Department of Chemistry, Purdue University, West Lafayette, Indiana 47907, United States and [‡]The Institute of Respiratory Diseases, Xinqiao Hospital, 183 Xingqiao Street, Chongqing 400037, China

ABSTRACT This paper reports a strategy for DNA self-assembly. Cross-over-based DNA nanomotifs are held together by T-junctions instead of commonly used sticky-end cohesion. We have demonstrated this strategy by assembling a DNA tetrahedron, an octahedron, and an icosahedron. The resulting DNA polyhedra contain out-pointing, short DNA hairpin spikes. These hairpins are well-structured relative to the polyhedra core and provide potential locations for introduction of functional chemicals such as proteins and gold nanoparticles. The T-linked DNA polyhedra have been characterized by polyacrylamide gel electrophoresis, atomic force microscopy, and dynamic light scattering.

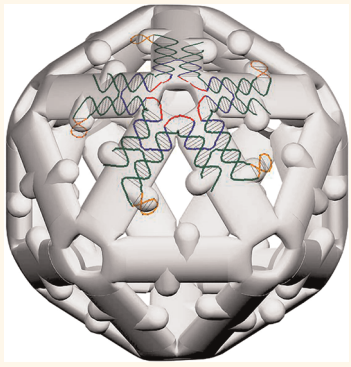

KEYWORDS: DNA · nanostructures · self-assembly · supramolecular chemistry · nanocages

Programmed DNA self-assembly provides an efficient method to prepare nanostructures.[1−3] A key component of the DNA self-assembly is sticky-end association, which holds multiple DNA nanomotifs (tiles) together to form large nanostructures.[4−12] It has been used for almost all multi-tile DNA assembly (other alternative strategies exist for nonrepetitive structures).[13−26] Upon assembly, the sticky-ends become integral parts of the frameworks of the resulting nanostructures. Any modification to the sticky-ends may interrupt the cohesion and introduce structural defects. For many applications, it is necessary to introduce structurally well-defined elements that are not integral parts of the overall frameworks. Such elements could provide locations to incorporate guests (*e.g.*, proteins, nanoparticles) with reduced motion freedom and great structural control. One noticeable exception to sticky-end association is a recently reported T-junction assembly (Figure 1a).[27] A T-junction consists of two DNA helices. One helix has an unpaired, single-stranded DNA loop at the middle (red), and the other helix has an unpaired, single-stranded tail (blue). These two single-stranded regions are complementary to each other. Their hybridization brings the two helices together to form a well-structured, T-shaped junction. This study inspired us to explore whether T-junctions can be used as cohesive bonds to bring cross-over-based DNA tiles together for assembly of large DNA nanostructures. As a test to this question, we have assembled a series of DNA polyhedra.

This work is partially built on our previous works of DNA polyhedra from sticky-ended, symmetric DNA star motifs.[28−31] In those polyhedra, all DNAs are integral elements of the polyhedra. There is no accessory DNA element that allows conjugation with other molecules/materials. One effort to overcome this problem is to introduce hairpins by a three-arm junction near the center of the star motif. With this strategy, we have assembled a spiked DNA tetrahedron.[32] However, the three-arm junctions are structurally ill-defined[33,34] and greatly increase the flexibility of the star motifs. Thus, it becomes very difficult to predict the tile flexibility, an essential factor for controlling the DNA self-assembly. The out-pointing hairpins are flexible relative to the tetrahedron frameworks. The current work has nicely addressed these problems.

The key of the reported strategy is to replace the sticky-ends with complementary T-junction pairs. In this design, an *n*-point star motif contains $n + 1$ strands: a central, long, repetitive DNA strand (**L*n***) with *n* sequence repeats and *n* copies of identical peripheral strand (**P**). The *n*-point star motif contains *n* identical branches that are related to each other by an *n*-fold rotational symmetry. All star motifs use the same peripheral strand (**P**) but different central strand (**L*n***) depending on the number of branches. Each branch is a four-arm junction. Its two outside arms contain a complementary T-junction pair. One of them has a single-stranded tail, and the other has a single-stranded internal loop.

* Address correspondence to wanggs2003@gmail.com, mao@purdue.edu.

Received for review February 23, 2012 and accepted May 6, 2012.

Published online May 06, 2012
10.1021/nn300813w

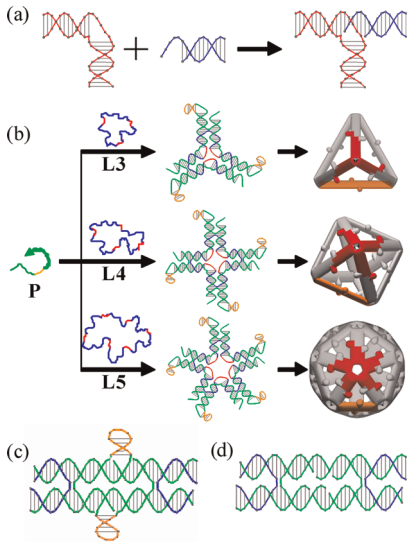

Figure 1. Self-assembly of spiked DNA polyhedra with T-junction linkages. (a) Formation of a structurally well-defined T-junction that joins a bulged DNA duplex (red) and a duplex (blue) with 5-base single-stranded overhang. (b) Self-assembly of spiked DNA tetrahedra from star-shaped DNA motifs (tiles). Each motif contains an L*n* strand and *n* copies of P strands. At the peripheral end of each branch of the star motif, there is a complementary T-junction pair: a single-stranded, 5-base-long overhang and a 5-base-long internal loop. T-junction interactions among the individual tiles would lead to the formation of DNA polyhedra. Each vertex of the polyhedra will be a DNA star motif, and one component star tile in each polyhedron is highlighted red. (c) Detailed structure of a strut [highlighted golden in the polyhedra shown in (b)] of the T-linked DNA polyhedra. There is a T-junction on each component of the DNA duplex. (d) Strut structure of the previously assembled, sticky-ended DNA polyhedra[28−31] is shown for comparison.

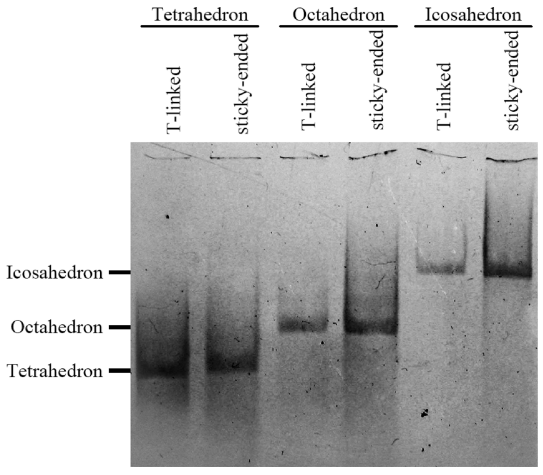

Figure 2. Native polyacrylamide gel electrophoresis (PAGE, 2.5%) analysis of the formation of T-linked DNA polyhedra. Well characterized, sticky-ended polyhedra were used as size markers.[28−30]

They are complementary to each other. When two star tiles interact with each other, two T-junctions will form between the two tiles. The two interacting branches from the two tiles consist of a strut (42 base pairs or 4 helical turns long) of the final DNA structures

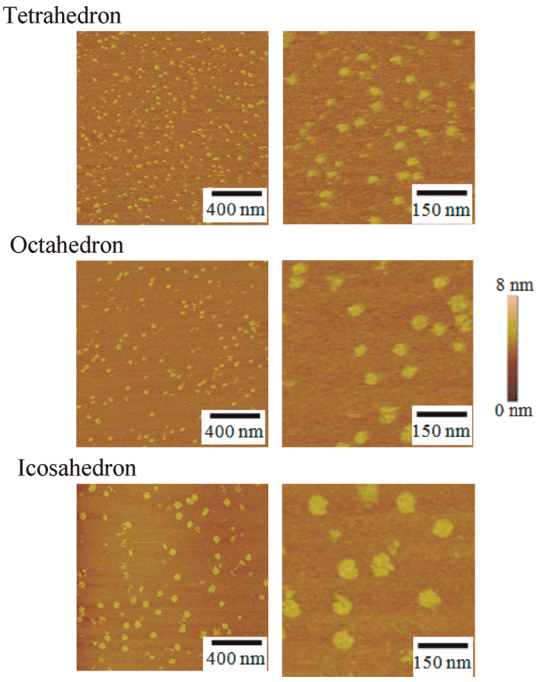

Figure 3. Atomic force microscopy (AFM) analysis of the T-linked DNA polyhedra. For each polyhedron, two images are presented at different imaging scales. All images have the same height scale as shown at the right.

(polyhedra). The two T-junctions are located roughly at the middle region of the strut. During the design, the positions of the T-junctions are carefully chosen to avoid steric crowdedness. The hairpins of the T-junctions are pointing to empty spaces instead of directly pointing any DNA duplexes. When compared with the DNA polyhedra assembled by traditional sticky-ends, the DNA polyhedra with T-junction have roughly the same physical size but with two additional hairpins on each strut.

RESULTS AND DISCUSSION

We followed previously reported DNA assembly protocol to assemble the T-linked DNA polyhedra.[4] For each polyhedron, two component DNA strands (**L*n***and **P**) were mixed at a ratio of 1:*n* in a Mg^{2+}-containing, neutral, aqueous buffer and slowly cooled from 95 to 25 °C over 2 days. Upon cooling, DNA strands recognized and associated with each other to form individual star-shaped tiles and then further assembled into DNA polyhedra through T-junction interactions (Figure 1b). The assembled T-linked spiked DNA polyhedra were first characterized by native polyacrylamide gel electrophoresis (PAGE). The well-characterized DNA polyhedra[28−30] assembled from sticky-end cohesion were used as size markers. For each type of polyhedron, the sticky-ended one and the new T-linked one had similar physical sizes and molecular weights. Hence, they should have similar electrophoretic mobilities. In the gel, the DNA complexes appeared as sharp single bands, indicating that the

assembly yields were high and the DNA complexes were stable. Furthermore, the DNA complexes had almost the same mobility as the sticky-ended polyhedra (Figure 2), demonstrating that the formed DNA complexes were the designed T-linked DNA polyhdedra.

We further characterized the T-linked DNA polyhedra with atomic force microscopy (AFM) and dynamic light scattering (DLS). Under AFM imaging, uniform-sized particles were observed (Figure 3), confirming that the assembly yields were high and the T-linked polyhedra were stable. It was also clear that the particles became larger and taller from tetrahedron, to octahedron, to icosahedron, as expected. DLS study measured the hydrodynamic radius of the DNA complexes. The DNA complexes indeed had the expected radii (Figure 4) assuming that the DNA duplex has a diameter of 2 nm and the rise is 0.33 nm per base pair, which further indicated the successful assembly of the T-linked DNA polyhedra.

An important application of the reported strategy is that the hairpins are not essential elements for the assembled polyhedra and can be easily replaced by other functional elements, such as aptamers (Figure 5). To demonstrate this notion, we replaced the short hairpins with a thrombin-binding DNA aptamer (colored golden).[35] We assembled an aptamer-tetrahedron, an aptamer-octahedron, and an aptamer-icosahedron and checked the assemblies by native PAGE (Figure 5a). Compared with a hairpin-polyhedron, the corresponding aptamer-polyhedron had a slightly higher molecular weight and larger physical size. Thus, the aptamer-polyhedra were expected to migrate slightly slower than the hairpin-polyhedra. The PAGE experiment confirmed the expectation and proved the successful assemblies of DNA polyhedra with aptamers through T-linkage. Furthermore, the anti-thrombin aptamer, after incorporated into the DNA polyhedra, retained its thrombin-binding activity. As shown in Figure 5b, an obvious mobility shift was observed for the DNA complex when incubated with thrombin. This experiment confirmed that the DNA polyhedral scaffold would not interfere with the 3D structure and binding property of the aptamer.

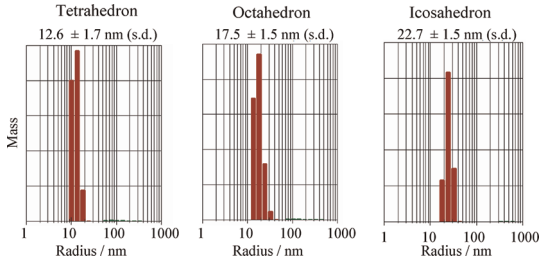

Figure 4. Dynamic light scattering (DLS) analysis of the T-linked DNA polyhedra. The measured hydrodynamic radii are shown on the corresponding graphs. The radii calculated from the DNA models are 12.6, 15.3, and 20.9 nm for the tetrahedron, octahedron, and icosahedron, respectively.

CONCLUSIONS

We have developed a general strategy to assemble DNA polyhedra with well-defined additional structural elements. Different from the reported strategy, it is quite easy to introduce additional, single-stranded tails to DNA polyhedra. Through hybridization, extra DNA components (*e.g.*, aptamers) can attach to the DNA polyhedra. It is simple and straightforward. However, such DNA components will be flexible relative to the DNA polyhedra, thus losing the structural control. Overall, it is an alternative strategy to the strategy reported in this work and might be useful to some

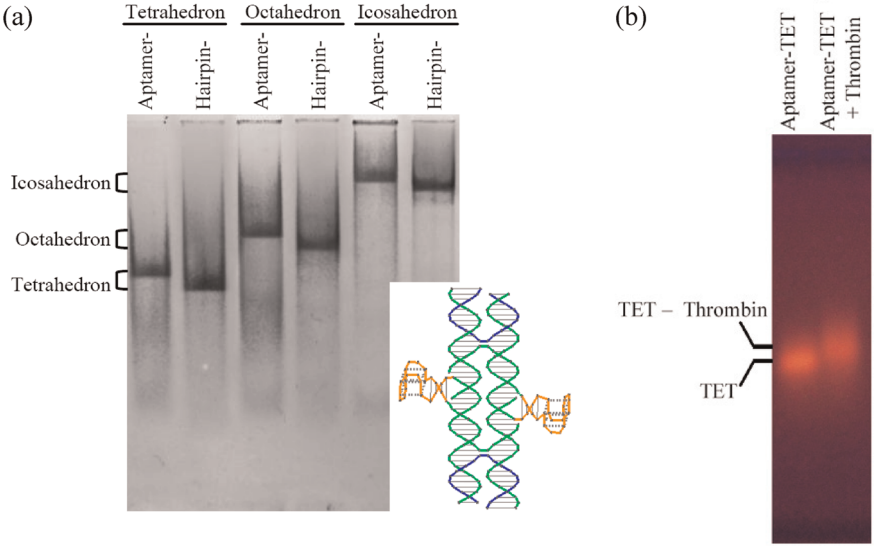

Figure 5. T-linked DNA polyhedra with anti-thrombin apatmers. (a) Native PAGE analysis of the aptamer-polyhedra. Lower right shows the detailed structure of the strut of the T-linked DNA polyhedra with thrombin apatmers (colored golden). (b) Gel shift experiment of thrombin binding of the aptamer-tetrahedron (TET) as analyzed by 1% agarose gel elecctrophoresis.

applications that do not require tight structural controls. The current work has also proven that T-junction can be used as a general cohesion method to assemble Holliday junction-based DNA motifs into large DNA architectures.

EXPERIMENTAL METHODS

Oligonucleotides. DNA sequences were adapted from previous works, which were originally designed by the SEQUIN computer program. All oligonucleotides were purchased from IDT and purified by 10−15% denaturing PAGE. DNA sequences:

strand **L3**: AGG CAC CAT CGT AGG TTT AAC TTG CCA GGC ACC ATC GTA GGT TTA ACT TGC CAG GCA CCA TCG TAG GTT TAA CTT GCC; strand **L4**: AGG CAC CAT CGT AGG TTT AAC TTG CCA GGC ACC ATC GTA GGT TTA ACT TGC CAG GCA CCA TCG TAG GTT TAA CTT GCC AGG CAC CAT CGT AGG TTT AAC TTG CC; strand **L5**: AGG CAC CAT CGT AGG TTT TTC TTG CCA GGC ACC ATC GTA GGT TTT TCT TGC CAG GCA CCA TCG TAG GTT TTT CTT GCC AGG CAC CAT CGT AGG TTT TTC TTG CCA GGC ACC ATC GTA GGT TTT TCT TGC C; strand **P**: GCT CGG CTC CCT GCC TGG CAA GCC TAC GAT GGA CAC GGT AAC CCG CCT TTT GGC GGC GAG CGT TAC CGT GTG GGA GC; strand **P'** (with aptamer): GCT CGG CTC CCT GCC TGG CAA GCC TAC GAT GGA CAC GGT AAC CCG CAG TCC GTG GTA GGG CAG GTT GGG GTG ACT GCG GCG AGC GTT ACC GTG TGG GAG C.

The color coding of the DNA sequences is the same as in Figure 1b,c. The aptamer sequence is underlined. For tetrahedron, 50 nM **L3** + 150 nM **P** (or **P**′); for octahedron, 50 nM **L4** + 200 nM **P** (or **P**′); for icosahedron, 20 nM **L5** + 100 nM **P** (or **P**′).

Formation of DNA Complexes. DNA strands were combined according to the indicated concentration in a Tris-acetic-EDTA-Mg^{2+} (TAE/Mg^{2+}) buffer (40 mM Tris base, 20 mM acetic acid, 2 mM EDTA, and 12.5 mM magnesium acetate). DNA assembly involved cooling solutions from 95 to 25 °C over 48 h. After assembly, DNA samples were directly used for AFM imaging and DLS study.

Native PAGE. Native PAGE containing 2.5% polyacrylamide was run on a FB-VE10-1 electrophoresis unit (FisherBiotech) at 4 °C (90 V, constant voltage) with TAE/Mg^{2+} buffer. The DNA samples were concentrated with Microcon YM-30 (30 kDa) Centrifugal filter units to ≈250 nM before electrophoresis. After electrophoresis, the gels were stained with Stains-All (Sigma) and scanned with a common office scanner.

Thrombin Binding Assay for Aptamer-Tetrahedra. Aptamer-tetrahedra (1 μg in 20 μL) were incubated with thrombin (Sigma) in TAE/Mg^{2+} buffer at 1:1 ratio at room temperature for 2 h. Nondenaturing agarose gel electrophoresis (1%) was run on a FB-SB-710 electrophoresis system (FisherBiotech) at 4 °C (60 V/8 cm, constant voltage) with TAE/Mg^{2+} buffer for 4 h. After electrophoresis, the gel was stained with ethidium bromide solution (10 μg/mL, 300 mL) for 3 h, distained in TAE/Mg^{2+} buffer (300 mL) for 2 h, and then photographed with iPhone 4S.

AFM Imaging. AFM was performed by tapping mode on a Multimode AFM with a Nanoscope IIIa controller (Veeco) using NP-S tips (Veeco) in air at room temperature.

DLS. DLS was carried out on a DynaPro 99 (Protein Solutions/Wyatt) with laser wavelength of 824 nm at 20 °C with 12 μL DNA sample.

Conflict of Interest: The authors declare no competing financial interest.

Acknowledgment. This work was supported by the Office of Naval Research and the National Science Foundation of China (No. 81028001).

REFERENCES AND NOTES

1. Seeman, N. C. DNA in a Material World. *Nature* **2003**, *421*, 427–431.
2. Lin, C.; Liu, Y.; Rinker, S.; Yan, H. DNA Tile Based Self-Assembly: Building Complex Nano-Architectures. *ChemPhysChem* **2006**, *7*, 1641–1647.
3. Feldkamp, U.; Niemeyer, C. M. Rational Design of DNA Nanoarchitectures. *Angew. Chem., Int. Ed.* **2006**, *45*, 1856–1876.
4. Winfree, E.; Liu, F.; Wenzler, L. A.; Seeman, N. C. Design And Self-Assembly of Two Dimensional DNA Crystals. *Nature* **1998**, *394*, 539–544.
5. Yan, H.; Park, S. H.; Finkelsterin, G.; Reif, J. H.; LaBean, T. H. DNA-Templated Self-Assembly of Protein Arrays and Highly Conductive Nanowires. *Science* **2003**, *301*, 1882–1884.
6. Wei, B.; Mi, Y. A New Triple Crossover Triangle (TXT) Motif for DNA Self-Assembly. *Biomacromolecules* **2005**, *6*, 2528–2532.
7. Rothemund, P. W. K.; Papadakis, N.; Winfree, E. Algorithmic Self-Assembly of DNA Sierpinski Triangles. *PloS Biol* **2004**, *2*, 2041–2053.
8. Liu, W.; Zhong, H.; Wang, R.; Seeman, N. C. Crystalline Two-Dimensional DNA-Origami Arrays. *Angew. Chem., Int. Ed.* **2011**, *50*, 264–267.
9. Hansen, M. N.; Zhang, A. M.; Rangnekar, A.; Bompiani, K. M.; Carter, J. D.; Gothelf, K. V.; LaBean, T. H. Weave Tile Architecture Construction Strategy for DNA Nanotechnology. *J. Am. Chem. Soc.* **2010**, *132*, 14481–14486.
10. He, Y.; Chen, Y.; Liu, H.; Ribbe, A. E.; Mao, C. Self-Assembly of Hexagonal DNA Two-Dimensional (2D) Arrays. *J. Am. Chem. Soc.* **2005**, *127*, 12202–12203.
11. He, Y.; Tian, Y.; Chen, Y.; Deng, Z.; Ribbe, A. E.; Mao, C. Sequence Symmetry as a Tool for Designing DNA Nanostructures. *Angew. Chem., Int. Ed.* **2005**, *44*, 6694–6696.
12. He, Y.; Tian, Y.; Ribbe, A. E.; Mao, C. Highly Connected Two-Dimensional Crystals of DNA Six-Point-Stars. *J. Am. Chem. Soc.* **2006**, *128*, 15978–15979.
13. Chen, J. H.; Seeman, N. C. Synthesis from DNA of a Molecule with the Connectivity of a Cube. *Nature* **1991**, *350*, 631–633.
14. Zhang, Y. W.; Seeman, N. C. Construction of a DNA-Truncated Octahedron. *J. Am. Chem. Soc.* **1994**, *116*, 1661–1669.
15. Shih, W. M.; Quispe, J. D.; Joyce, G. F. A 1.7-Kilobase Single-Stranded DNA That Folds into a Nanoscale Octahedron. *Nature* **2004**, *427*, 618–621.
16. Goodman, R. P.; Schaap, A. T.; Tardin, C. F.; Erben, C. M.; Berry, R. M.; Schmidt, C. F.; Turberfield, A. J. Rapid Chiral Assembly of Rigid DNA Building Blocks for Molecular Nanofabrication. *Science* **2005**, *310*, 1661–1665.
17. Douglas, S. M.; Dietz, H.; Liedl, T.; Högberg, B.; Graf, F.; Shih, W. M. Self-Assembly of DNA into Nanoscale Three-Dimensional Shapes. *Nature* **2009**, *459*, 414–418.
18. Kuzuya, A.; Komiyama, M. Design and Construction of a Box-Shaped 3D-DNA Origami. *Chem. Commun.* **2009**, 4182–4184.
19. Andersen, E. S.; Dong, M.; Nielsen, M. M.; Jahn, K.; Subramani, R.; Mamdouh, W.; Golas, M. M.; Sander, B.; Stark, H.; Oliveira, C. L. P. Self-Assembly of a Nanoscale DNA Box with a Controllable Lid. *Nature* **2009**, *459*, 73–76.
20. Ke, Y. G.; Sharma, J.; Liu, M. H.; Jahn, K.; Liu, Y.; Yan, H. Scaffolded DNA Origami of a DNA Tetrahedron Molecular Container. *Nano Lett.* **2009**, *9*, 2445–2447.
21. Afonin, K.; Bindewald, E.; Yaghoubian, A. J.; Voss, N.; Jacovetti, E.; Shapiro, B. A.; Jaeger, L. *In Vitro* Assembly of Cubic RNA-Based Scaffolds Designed *in Silico*. *Nat. Nanotechnol.* **2010**, *5*, 676–682.
22. Aldaye, F. A.; Sleiman, H. F. Modular Access to Structurally Switchable 3D Discrete DNA Assemblies. *J. Am. Chem. Soc.* **2007**, *129*, 13376–13377.
23. Bhatia, D.; Mehtab, S.; Krishnan, R.; Indi, S. S.; Basu, A.; Krishnan, Y. Icosahedral DNA Nanocapsules by Modular Assembly. *Angew. Chem., Int. Ed.* **2009**, *48*, 4134–4137.
24. Andersen, F. F.; Knudsen, B.; Oliveira, C. L. P.; Frøhlich, R. F.; Krüger, D.; Bungert, J.; Agbandje-McKenna, M.; McKenna, R.; Juul, S.; Koch, J.; *et al.* High-Yield Assembly of a Stable Nanoscale DNA Cage. *Nucleic Acids Res.* **2008**, *36*, 1113–1119.
25. Zimmermann, J.; Cebulla, M. P. J.; Mönninghoff, S; von Kiedrowski, G. Self-Assembly of a DNA Dodecahedron from 20 Trisoligonucleotides with C3h Linkers. *Angew. Chem., Int. Ed.* **2008**, *47*, 3626–3630.

26. Lundberg, E. P.; Plesa, C.; Wilhelmsson, L. M.; Lincoln, P.; Brown, T.; Nordén, B. Nanofabrication Yields. Hybridization and Click-Fixation of Polycyclic DNA Nanoassemblies. *ACS Nano* **2011**, *5*, 7565–7575.
27. Hamada, S.; Murata, S. Substrate-Assisted Assembly of Interconnected Single-Duplex DNA Nanostructures. *Angew. Chem., Int. Ed.* **2009**, *48*, 6820–6823.
28. He, Y.; Ye, T.; Su, M.; Zhang, C.; Ribbe, A. E.; Jiang, W.; Mao, C. Hierarchical Self-Assembly of DNA into Symmetric Supramolecular Polyhedra. *Nature* **2008**, *452*, 198–201.
29. He, Y.; Su, M.; Fang, P.; Zhang, C.; Ribbe, A. E.; Jiang, W.; Mao, C. On the Chirality of Self-Assembled DNA Octahedra. *Angew. Chem., Int. Ed.* **2010**, *49*, 748–751.
30. Zhang, C.; Su, M.; He, Y.; Zhao, X.; Fang, P.; Ribbe, A. E.; Jiang, W.; Mao, C. Conformational Flexibility Facilitates Self-Assembly of Complex DNA Nanostructures. *Proc. Natl. Acad. Sci. U.S.A.* **2008**, *105*, 10665–10669.
31. Zhang, C.; Ko, S. H.; Su, M.; Leng, Y.; Ribbe, A. E.; Jiang, W.; Mao, C. Symmetry Controls the Face Geometry of DNA Polyhedra. *J. Am. Chem. Soc.* **2009**, *131*, 1413–1415.
32. Zhang, C.; Su, M.; He, Y.; Leng, Y.; Ribbe, A. E.; Wang, G.; Jiang, W.; Mao, C. Exterior Modification of a DNA Tetrahedron. *Chem. Commun.* **2010**, *46*, 6792–6794.
33. Duckett, D. R.; Lilley, D. M. The Three-Way DNA Junction Is a Y-Shaped Molecule in Which There Is No Helix−Helix Stacking. *EMBO J.* **1990**, *9*, 1659–1664.
34. Leontis, N. B.; Kwok, W.; Newman, J. S. Stability and Structure of Three-Way DNA Junctions Containing Unpaired Nucleotides. *Nucleic Acids Res.* **1991**, *19*, 759–766.
35. Ellington, A. D.; Szostak, J. W. *In Vitro* Selection of RNA Molecules That Bind Specific Ligands. *Nature* **1990**, *346*, 818–822.